

Morphological and electrical properties of Ag/p-type indium phosphide MIS structures with malachite green organic dyes

S. Asubay^a, C. A. Ava^b, O. Gullu^{c,*}

^aDicle University, Faculty of Sciences, Department of Physics, Diyarbakir, Turkey

^bDicle University, Science and Technology Application and Research Center, DÜBTAM Laboratories, Diyarbakir, Turkey

^cBatman University, Faculty of Sciences and Arts, Department of Physics, Batman, Turkey

Malachite Green (MG) organic dye thin film was prepared by simple drop casting method. Microstructural property of MG layer was investigated by Scanning Electron Microscopy (SEM). SEM image indicated that MG organic thin layer was formed from nanoclusters. Later, it was fabricated Ag/Malachite Green(MG)/p-InP diodes by drop cast method. The barrier height (BH) and ideality factor by using I-V characteristics for the device were found as 0.75 eV and 1.68. By using the Norde method, the BH and the resistance of neutral region of the device were extracted as 0.80 eV and $1.17 \times 10^4 \Omega$. The interfacial states concentration of the device has been seen to decrease from $2.79 \times 10^{13} \text{ eV}^{-1} \text{ cm}^{-2}$ to $5.80 \times 10^{12} \text{ eV}^{-1} \text{ cm}^{-2}$. By using capacitance-voltage technique, the values of the built-in voltage, BH and semiconductor doping density were found as 1.22 V, 0.83 eV and $1.87 \times 10^{17} \text{ cm}^{-3}$ for the Ag/MG/p-InP diode, respectively.

(Received March 11, 2022; Accepted June 3, 2022)

Keywords: MIS diode, Interface states, Series resistance, Malachite green

1. Introduction

The organic solids have been employed widely because of durability and barrier modification effects in the metal/interfacial film/semiconductor (MIS) junctions [1-14]. For example, the basic diode parameters of metal/semiconductor (MS) junctions could be adjusted by organic interlayer. Padma et al. [3] used a polyethylene oxide (PEO) molecule as an interface sheet to modify electronic property of the Titanium/p-type Indium Phosphide structure. The junctions were characterized by current-voltage (I-V) and capacity-voltage-frequency (C-V-f) measurements. Padma et al. [3] reported that the ideality factor (n) and barrier height (BH) were obtained as 0.74 eV and 0.84 eV for the diodes without and with PEO layer. Sreenu et al. [5] performed the electrical characteristics of Ti/Orange G (OG)/p-InP structures. They [5] found the values of the BH as 0.83 eV and 0.94 eV for the conventional contact without OG layer and Ti/OG/p-InP contact with OG layer. Reddy et al. [7] produced the Ti/polyvinylpyrrolidone (PVP)/p-InP structure. Reddy et al. [7] calculated the values of BH as 0.76 eV and 0.87 eV for the contacts without and with PVP layer. Sekhar Reddy et al. [9] fabricated the Ti/p-InP contacts with and without polyaniline (PANI) interfacial layer. They [9] extracted as 0.81 eV and 0.64 eV the BHs for the contacts with and without PANI interfacial thin layer. Aydogan et al. [10] fabricated the Al/aniline green (AG)/Ga₂Te₃ diode with AG thin layer. The parameters of the n and BH from I-V measurement of Al/aniline green (AG)/Ga₂Te₃ junction were found as 1.79 and 0.67 eV. Güllü et al. [13] identically produced the Al/AG/p-Si diodes (total 27 contacts) by using drop cast method onto a p-type Silicon substrate. It was reported that mean BH and n from the current-voltage plots were extracted as 0.582 eV and 2.999, respectively. They [13] found that the mean BH and mean acceptor carrier density of semiconductor from C-V characteristics were extracted as 0.61 eV and $5.54 \times 10^{14} \text{ cm}^{-3}$. Aydogan et al. [15] performed the electrical measurements of AG/n-Silicon diode. They calculated as 3.48 and 0.76 eV the parameters of the n and BH extracted

* Corresponding author: omergullu@gmail.com

<https://doi.org/10.15251/JOR.2022.183.421>

from current–voltage characteristics, respectively. The different electrical features of the MS junctions might be changed with selecting of appropriate material [15]. In this work, we have considered the malachite green or aniline green (MG) organic molecule because of the property of chemical stability in different electronics and photo-electronic technology [16]. This material gives an opportunity of cheap and huge-surface semiconductor junctions. MG with chemical formula $C_{23}H_{25}ClN_2$ employed in this work is a conventional aromatic azo dye molecule as shown the molecular structure in Figure 1.

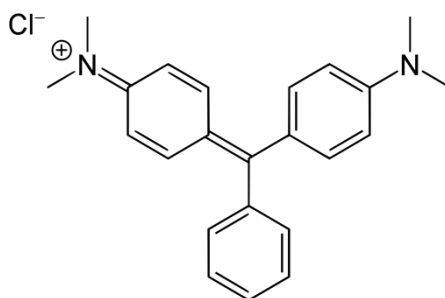


Fig. 1. The molecular structure of MG molecule.

This work aims to analyze the electronic and interfacial characteristics of Ag/MG/p-InP/Au-Zn device with the joint of MG thin film between the indium phosphide inorganic substrate and Ag top metal layer. The electronic properties of the Ag/MG/p-InP device were extracted by using I-V and C-V techniques.

2. Experimental procedure

Ag/MG/p-InP MIS diode structures were formed on the p-type InP crystal. The chemical cleaning procedure of the semiconductor p-InP substrate was performed with $5H_2SO_4 + H_2O_2 + H_2O$ solution. A $HF+10H_2O$ suspension was utilized to etch the ultrathin oxide layer on p-InP wafer and then the p-InP substrate was cleaned in the deionized (DI) water. The 90: Au–10: Zn alloy to form of the back metal contact of the p-InP wafer was evaporated in thermal evaporation system. Then, thermal annealing procedure was applied to the wafer at 450 °C for three minutes in nitrogen chamber. MG organic layer on the p-InP crystal was fabricated by dropping 10 μ L of the MG solution. Then, it was left by itself for evaporation of ethanol for two hours. Ag metal top contact with diameter of 1.0 mm on the organic film was created by evaporating pure Ag material (diode surface area = $78.5 \times 10^{-4} \text{ cm}^2$). All thermal coating stages in this study were performed in a vacuum chamber at 2×10^{-5} Torr. Electrical measurements of the Ag/MG/p-InP/Au-Zn device as shown in Figure 2 were taken by Keithley 4200 SCS analysis system at 300 K and under darkness. The structural properties of the MG organic dye layer coated on glass substrate were investigated by Quanta FEG 250 Scanning Electron Microscopy (SEM) system.

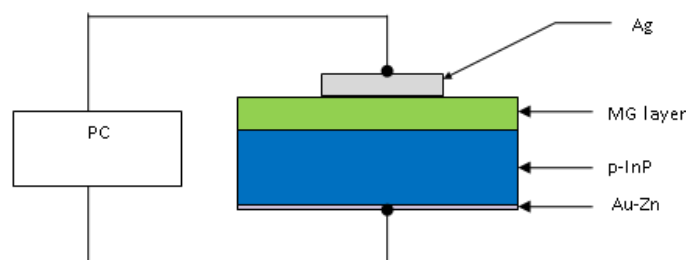


Fig. 2. The experiment setup of the Ag/MG/p-InP/Au-Zn MIS contact structure.

3. Results and Discussion

3.1. The morphological characteristics of the MG film

The morphological properties of organic thin films, which play an active role on the performance of opto-electronic devices, are as seen in the figure. The morphological characteristics of the MG organic dye thin layer coated on glass substrate were investigated by SEM measurement. The SEM results of the MG layer are indicated in Figure 3 (a,b). As indicated in Figure 3a, the MG organic thin layer is formed from nanoclusters. The cluster size of the layer was found to be in the range of 300-450 nm as seen in Fig. 3b.

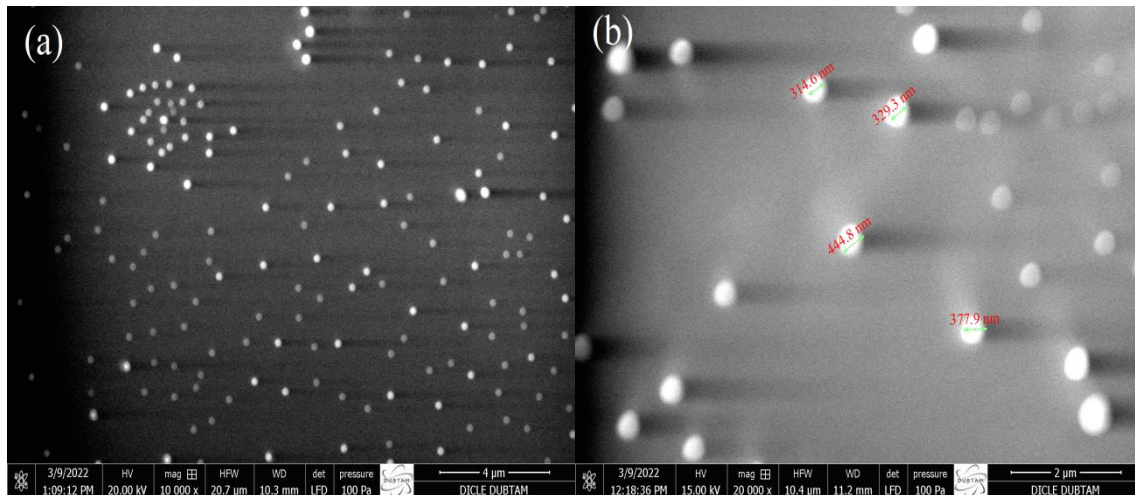


Fig. 3. a) Low magnification and b) high magnification SEM photomicrographs of the MG layer.

3.2. The I-V graphics of the Ag/MG/p-InP contact

The I - V graphics of the Ag/MG/p-InP contact and Ag/p-InP conventional contact have been drawn in Figure 4. MG thin film layer decreases the diode current of the Ag/p-InP conventional contact as seen in Figure 4. The Ag/MG/p-InP MIS diode displays a rectifying character. The diode current in forward-bias region at higher current section of the $\log I$ - V plot was in control of series resistance. Then it gives rise to the curvature in $\log I$ - V graphic. The parameters of n and BH (Φ_b) from thermionic emission (TE) mechanism [17,18] were computed from straight section of the I - V graphic of the diode. The Φ_b and n for Ag/MG/p-InP/Au-Zn MIS device were obtained as 0.75 eV and 1.68. The value of n extracted by the Schottky effect only can be near to 1.01 or 1.02 [19-21]. The greater values of n are ascribed to consequent influences which count in the interfacial dipoles because of the MIS interfacial characteristics or interfacial doping as well as the defects due to fabrication process at the interfacial layer [19-22]. Tung et al [22] also ascribed the great values of n to the existence of a broad arrangement of small-potential patches due to the side-by-side inhomogeneities at MIS interface.

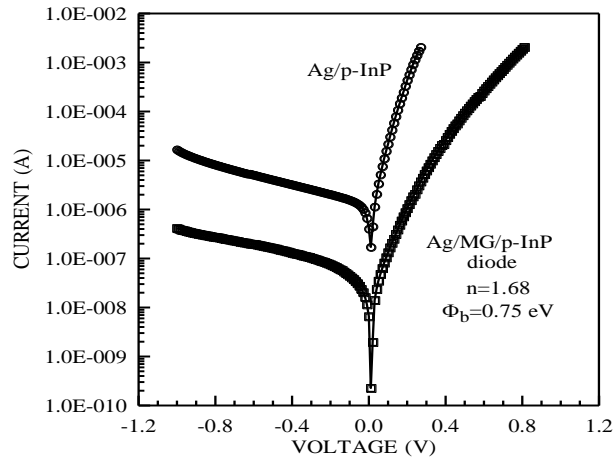


Fig. 4. Current-Voltage graphics of the Ag/MG/p-InP/Au-Zn contact and Ag/p-InP contact.

The parameter of Φ_b of 0.75 eV determined for the device with MG thin interlayer is greater than the value of 0.64 eV extracted for control diode. The experimental studies reported by many researchers have shown the modification of the BH with utilization of the various organic molecules. D. R. Lambada et al. [23] produced the Au/graphene oxide (GO)/p-InP MIS contact with GO thin layer. They calculated as 1.67 and 0.87 eV the n and BH of the device in the dark. Also, Lin et al. [24] were fabricated the MoS₂/p-InP MIS contact. The BH, n and R_s by utilizing from I-V graphics were determined as 0.73 eV, 2.4, and 12.8 ohm. Chen et al. [25] produced the Al/MoO₃/p-InP contact structure and performed its diode characteristics with temperatures from 310 to 400 K. They showed that the parameters of the apparent Φ_b for the device were changed from about 0.78eV to 0.91 eV.

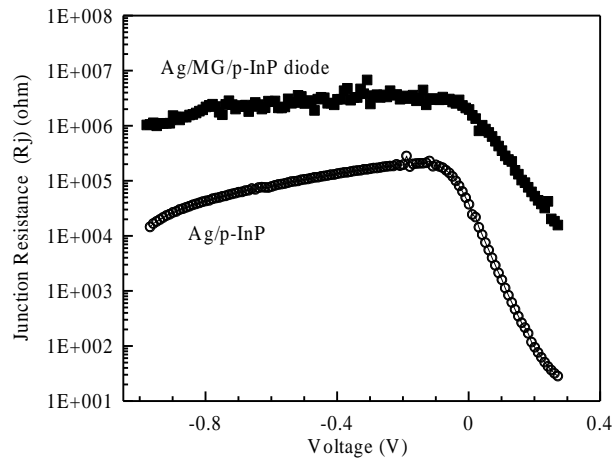


Fig. 5. R_j -V graphics of the Ag/MG/p-InP/Au-Zn contact and Ag/p-InP control contact.

They [23-25] have shown that the calculated BHs for these contacts were higher than the metal/p-InP control diodes. They [23-25] have reported that the BH might be changed or organized by using organic interlayer film. Also, this may be attributed to the organic thin layer that changes the Φ_b by affecting the depletion section of the semiconductor wafer [23-25]. The diode parameters obtained in this work and earlier works have indicated that the coating technique of the thin layer and the layer width of the material to be employed in MIS diode production influence the diode properties.

The junction resistance (R_j , $R_j = \partial V / \partial I$)-V graphics of the Ag/MG/p-InP structure and Ag/p-InP reference diode have been drawn in Figure 5. MG thin film layer increases to the diode resistance of the Ag/p-InP contact as seen in Figure 5.

The series resistance (R_s) effect causes to a convexity at higher potential region of the I-V curves [32]. R_s parameter has been extracted by help the Cheung technique [33,34]. The I-V equation of a MS contact by the R_s effect according to Cheung technique [34] may be formulated as:

$$I = I_0 \exp\left[\frac{q(V - IR_s)}{nkT}\right]. \quad (1)$$

The R_s value of the device may be extracted from the next expressions by help the Eq.(1);

$$\frac{dV}{d(\ln I)} = \frac{nkT}{q} + IR_s, \quad (2)$$

$$H(I) = n\Phi_b + IR_s, \quad (3)$$

A $\frac{dV}{d(\ln I)}$ -I graphic has to be straight line as shown in Fig.6. This curve provides R_s

value as the slope and $\frac{nkT}{q}$ as the y-axis intercept from Eq.(2). The parameters of n and R_s of

Ag/MG/p-InP MIS diode were extracted as $n = 2.15$ and $R_s = 45.9 \Omega$. It was seen that the parameter of n calculated from the $\log I$ -V curve was different from that determined from the $dV/d(\ln I)$ -I graphic. This situation may be ascribed to the influence of the R_s and interfacial charge states and to the potential falling through the interface region (native oxide + MG layer) [35]. Also, $H(I)$ -I graphic as given in Fig.6 has to be in a form of straight line according to the Cheung model [34] and then Φ_b and R_s are computed as 0.74 eV and 109.2 ohm.

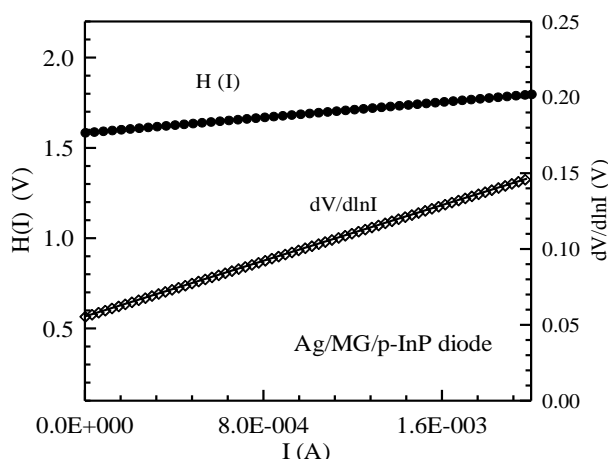


Fig. 6. The curves of Cheung functions of the Ag/MG/p-InP MIS device.

Norde developed a Norde function ($F(V)$) to extract the value of the R_s [36]. The value of BH by using the Norde function may be calculated from Eq. (4),

$$\Phi_b = F(V_0) + \frac{V_0}{\gamma} - \frac{kT}{q} \quad (4)$$

where γ is integer, $F(V_0)$ and V_0 is the bottom of $F(V)$ graph and the related potential, respectively. Figure 7 displays the $F(V)$ – V graphic of the Ag/MG/p-InP device. By utilizing the $F(V)$ – V curve as shown in Fig.7 it was obtained as the values of $F(V_0)=0.73$ Volt and $V_0=0.20$ Volt. Then, the BH and R_s for the Ag/MG/p-InP/Au-Zn MIS contact were extracted as 0.80 eV and $1.17 \times 10^4 \Omega$. It is noted which the barrier heights calculated from the $\log I$ – V method, Cheung technique and Norde technique are not similar to each other. These different values emerge from the calculation of various sections of the I – V graphics [37]. Thus, the R_s value extracted from Norde technique is larger than that extracted from Cheung technique. The diode parameters are calculated from the series resistance region in higher section of the $\log I$ – V graphics in the Cheung method, while they are extracted from the full forward bias section of the $\log I$ – V curves of the MIS structures in the Norde's technique [37]. The higher values of the ideality factor might increase the R_s value of the junction. Thus, the R_s value is higher for this contact. This shows that the R_s parameter is a current-restricting component for this MIS diode. The large R_s values might be attributed to reduce of the logarithmically rising rate in diode current because of space-charge injection into the MG interlayer at larger forward bias voltage section [37].

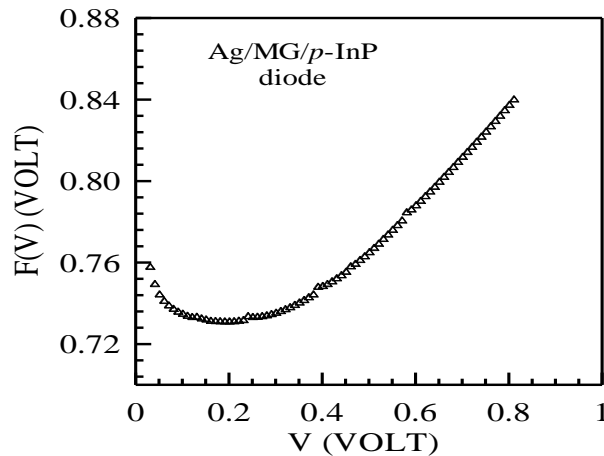


Fig. 7. F – V graphic of Ag/MG/p-InP MIS contact.

3.3. Interfacial analysis of the Ag/MG/p-InP contact

Card and Rhoderick [38] developed for the calculation of interfacial states concentration N_{SS} of a semiconductor junction and the energy of the interfacial states E_{SS} . The parameters of N_{SS} and E_{SS} according to the Ref.[38] were computed from the I – V data of the diodes and then the N_{SS} vs. E_{SS} – E_V graphics were drawn as given in Fig. 8. It is shown that N_{SS} values reduces with raising E_{SS} – E_V values for both Ag/p-InP reference diode and Ag/MG/p-InP diode. The interfacial state density values of the Ag/p-InP diode and Ag/MG/p-InP contact vary from $1.87 \times 10^{12} \text{ eV}^{-1} \text{ cm}^{-2}$ and $1.07 \times 10^{13} \text{ eV}^{-1} \text{ cm}^{-2}$ to $4.41 \times 10^{11} \text{ eV}^{-1} \text{ cm}^{-2}$ and $4.33 \times 10^{12} \text{ eV}^{-1} \text{ cm}^{-2}$, respectively. The increase in the interfacial state density values of Ag/MG/p-InP MIS contact is attributed to effect of the MG organic thin interlayer. Recently, Acar et al. [39] formed the Au/ZnO/p-InP junction and they reported that N_{SS} interface states changed from 8.18×10^{13} to $1.24 \times 10^{11} \text{ eV}^{-1} \text{ cm}^{-2}$ as a function of signal frequency. Lambada et al [23] found that N_{SS} values varied from $3.3629 \times 10^{16} \text{ eV}^{-1} \text{ cm}^{-2}$ to $4.0248 \times 10^{15} \text{ eV}^{-1} \text{ cm}^{-2}$ in the dark for Au/GO/p-InP diode. Sreenu et al. [5] found that the N_{SS} values varied from $3.731 \times 10^{12} \text{ eV}^{-1} \text{ cm}^{-2}$ to $6.637 \times 10^{11} \text{ eV}^{-1} \text{ cm}^{-2}$ for Ti/OG/p-InP diode. Ulasan et al [40] found that the N_{SS} values varied from $5.6 \times 10^{13} \text{ eV}^{-1} \text{ cm}^{-2}$ to $2.0 \times 10^{12} \text{ eV}^{-1} \text{ cm}^{-2}$ for Au/Si₃N₄/p-GaAs junction. Yilmaz et al [41] reported that N_{SS} values decreased from $4.268 \times$

$10^{15} \text{ eV}^{-1} \text{ cm}^{-2}$ to $1.587 \times 10^{15} \text{ eV}^{-1} \text{ cm}^{-2}$ in the dark condition for Au/*Pinus brutia*/n-Si MIS diode. The N_{ss} values of interfacial state concentration of the Ag/MG/p-InP MIS contact is coherent with those of above indicated works. The MG film layer results in a significant alteration of interface state that the MIS interface is sharp and passive [41-43]. The MG interlayer raises the BH by the alteration of the crystal substrate surfaces and the chemical interactions at the MIS interfacial region. The MG interlayer will produce new interfacial charge states between the p-InP and oxide-organic interfacial layer [7].

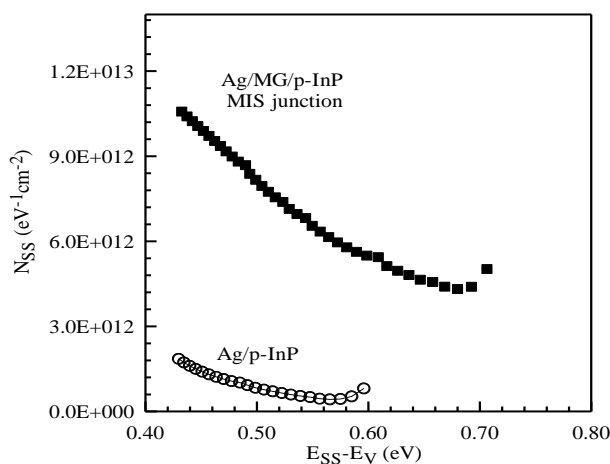


Fig. 8. The density distributions of the interfacial charge states of the Ag/p-InP/Au-Zn control diode and the Ag/MG/p-InP/Au-Zn device.

3.4. Capacity-Voltage Analysis of Ag/MG/p-InP/Au-Zn diodes

The C-V characteristics can ensure valuable understanding about the immobile charge distribution and BH of the diodes. When any voltage is applied to the diode, a capacitance occurs due to the change of the charge distribution within the structure. The depletion capacitance in the junction prevails in the reverse-bias region, while the diffusion capacitance prevails in large forward-bias region [44].

Figure 9 displays the C-V and $1/C^2$ -V curves of the Ag/MG/p-InP diode. The $1/C^2$ -V curve is straight which shows the configuration of Schottky contact [45]. By utilizing Mott-Schottky equation in C-V analysis [17,18] the values of the built-in potential (V_d), BH and semiconductor doping concentration (N_A) were found as 1.22 V, 0.83 eV and $1.87 \times 10^{17} \text{ cm}^{-3}$ for the Ag/MG/p-InP diode, respectively.

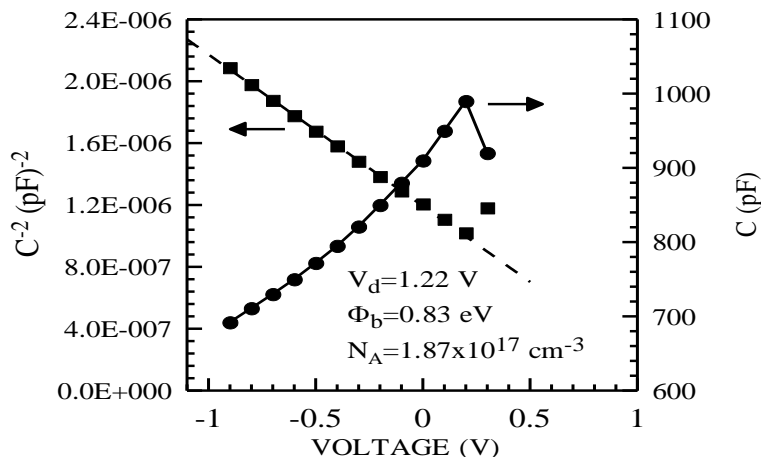


Fig. 9. The C-V and $1/C^2$ -V graphics at 1 MHz frequency for the Ag/MG/p-InP/Au-Zn device.

The different measurement mechanisms of the I-V and C-V characteristics for the Ag/MG/p-InP device cause to the difference in the extracted BH values. The capacity C is not precise to potential alteration on a distance magnitude of smaller than the depletion part and C-V technique measures the average BH over the whole depletion region. The junction current changes by the logarithmic function of BHs and thus depend precisely on the comprehensive distribution at the interfacial layer. Besides, the difference in the extracted Φ_b values of the diodes might be described by the presence of the interlayer and trap/defect states in bulk crystal wafer [17,18,46,47].

4. Conclusion

In conclusion, the morphological characteristics of the MG organic dye thin layer coated on glass substrate were investigated by SEM measurement. It was seen the MG organic thin layer is formed from nanoclusters. The cluster size of the layer was found to be in the range of 300-450 nm. Later, it was produced the Ag/MG/p-InP junction by simple drop casting technique. The Ag/MG/p-InP structure represents a rectifier property. The BH and n by using I-V measurements for the Ag/MG/p-InP junction were found as 0.75 eV and 1.68. By using the Norde method, the values of BH and series resistance (R_s) of the Ag/MG/p-InP structure were extracted as 0.80 eV and $1.17 \times 10^4 \Omega$, respectively. The interfacial states concentration of the Ag/MG/p-InP contact has been seen to vary from $2.79 \times 10^{13} \text{ eV}^{-1} \text{ cm}^{-2}$ to $5.80 \times 10^{12} \text{ eV}^{-1} \text{ cm}^{-2}$. By using the $1/C^2$ -V analysis, the values of the built-in voltage, BH and semiconductor doping concentration were found as 1.22 V, 0.83 eV and $1.87 \times 10^{17} \text{ cm}^{-3}$ for the Ag/MG/p-InP diode, respectively.

References

- [1] S.V. Frolov, M. Liess, P.A. Lane, W. Gellermann, Z.V. Vardeny, M. Ozaki, K. Yoshino, Phys. Rev. Lett., 78 (1997), p. 4285; <https://doi.org/10.1103/PhysRevLett.78.4285>
- [2] Z. Gadjourova, Y.G. Andreev, D.P. Tunstall, P.G. Bruce, Nature, 412 (2001), p. 520; <https://doi.org/10.1038/35087538>
- [3] R.Padma, K. Sreenu, V.Rajagopal Reddy, Journal of Alloys and Compounds Volume 695, 25 February 2017, Pages 2587-2596; <https://doi.org/10.1016/j.jallcom.2016.11.165>
- [4] N.S. Sariciftci, D. Braun, C. Zhang, V.I. Srdanov, A.J. Heeger, G. Stucky, F. Wudl, Appl. Phys. Lett., 62 (1993), p. 585; <https://doi.org/10.1063/1.108863>
- [5] K. Sreenu, C. Venkata Prasad, and V. Rajagopal Reddy, Journal of Electronic Materials, Vol. 46, No. 10, 2017; <https://doi.org/10.1007/s11664-017-5611-9>
- [6] W. C. Huang, T.C. Lin, C.T. Horng, C.C. Chen, Microelectronic Eng. 107 (2013) 200. <https://doi.org/10.1016/j.mee.2012.09.003>
- [7] M. Siva Pratap Reddy, K. Sreenu, V. Rajagopal Reddy, Chinho Park, Journal of Materials Science: Materials in Electronics volume 28, pages 4847-4855 (2017); <https://doi.org/10.1007/s10854-016-6131-8>
- [8] R. K. Gupta, R. A. Singh, Materials Chemistry and Physics 86 (2004) 279; <https://doi.org/10.1016/j.matchemphys.2004.03.003>
- [9] P. R. Sekhar Reddy, V. Janardhanam, I. Jyothi, Shim-Hoon Yuk, V. Rajagopal Reddy, Jae-Chan Jeong, Sung-Nam Lee, and Chel-Jong Choi Journal of Semiconductor Technology and Science, Vol.16, NO.5, October, 2016
- [10] Ş. Aydoğan and O. Gullu, Microelectronic Engineering Volume 87, Issue 2, February 2010, Pages 187-191; <https://doi.org/10.1016/j.mee.2009.07.007>
- [11] Ş. Aydoğan, M. Sağlam, A. Türüt, Y. Onganer, Mater. Sci. Eng.: C, 29 (2009), p. 1486; <https://doi.org/10.1016/j.msec.2008.12.006>
- [12] Phan DT, Gupta RK, Chung GS, Al-Ghamdi AA, Al-Hartomy OA, El-Tantawy F,

- Yakuphanoglu F (2012). Sol Energy 86(10):2961-2966;
<https://doi.org/10.1016/j.solener.2012.07.002>
- [13] Ö. Güllü, M. Biber and A. Türüt Journal of Materials Science: Materials in Electronics volume 19, pages 986-991 (2008); <https://doi.org/10.1007/s10854-007-9431-1>
- [14] S. Antohe, N. Tomozeiu, S. Gogonea, Phys. Stat. Sol. A 125 (1991) 397;
<https://doi.org/10.1002/pssa.2211250138>
- [15] Ş. Aydoğan Ö. Güllü A. Türüt Materials Science in Semiconductor Processing Volume 11, Issue 2, April 2008, Pages 53-58; <https://doi.org/10.1016/j.mssp.2008.11.004>
- [16] O. Gullu., O. Baris, M. Biber, A. Turut, Applied Surface Science 254 (2008) 3039;
<https://doi.org/10.1016/j.apsusc.2007.10.082>
- [17] H. K. Henisch, Semiconductor Contacts: An Approach to Ideas and Models, Clarendon Press, Oxford (1984).
- [18] B. L. Sharma, in: Semiconductors and Semimetals, Vol. 15, Academic Press, New York (1981)
- [19] Wang R, Xu M, Ye PD, Huang R. Journal of Vacuum Science & Technology B. 2011 Jul 1;29(4):041206; <https://doi.org/10.1116/1.3610972>
- [20] S. Gupta, P. Paramahans Manik, R. Kesh Mishra, A. Nainani, M.C. Abraham, S. Lodha J Appl Phys, 113 (23) (2013), Article 234505; <https://doi.org/10.1063/1.4811340>
- [21] H. Tecimer, A. Türüt, H. Uslu, Ş. Altındal, İ. Uslu, Sens Actuators, A, 1 (199) (2013), pp. 194-201; <https://doi.org/10.1016/j.sna.2013.05.027>
- [22] R. T. Tung, Phys. Rev. B 45(23) (1992) 13509; <https://doi.org/10.1103/PhysRevB.45.13509>
- [23] D. R. Lambada, S. Yang, Y. Wang, P. Ji, S. Shafique, F. Wang Nanomanufacturing and Metrology volume 3, pages 269-281 (2020); <https://doi.org/10.1007/s41871-020-00078-z>
- [24] Lin S, Peng W, Li X, Wu Z, Xu Z, Zhang S, Xu W (2015) Appl Phys Lett 9 (7):666.
- [25] Chen J, Wang Q, Lv J (2016) Thin Solid Films 616:145-150;
<https://doi.org/10.1016/j.tsf.2016.08.019>
- [32] Aydogan S, Saglam M, Turut A, Onganer Y (2009) Mater Sci Eng, C 29(4):1486-1490;
<https://doi.org/10.1016/j.msec.2008.12.006>
- [33] Şahin B, Çetin H, Ayyildiz E (2005) Solid State Commun 135(8):490-495;
<https://doi.org/10.1016/j.ssc.2005.05.050>
- [34] S. K. Cheung, N. W. Cheung, Appl. Phys. Lett. 49 (1986) 85; <https://doi.org/10.1063/1.97359>
- [35] Çaldıran, Z., Deniz, A. R., Aydoğan, Ş., Yesildag, A. and Ekinçi, D. (2013). Superlattices and Microstructures, 56, 45-54; <https://doi.org/10.1016/j.spmi.2012.12.004>
- [36] Norde, H. (1979). Journal of Applied Physics, 50, 5052;
<https://doi.org/10.1063/1.325607>
- [37] O. Gullu, S. Aydogan, A. Turut, Microelectronic Eng. 85 (2008) 1647;
<https://doi.org/10.1016/j.mee.2008.04.003>
- [38] H. C. Card, E. H. Rhoderick, J. Phys. D: Appl. Phys. 4 (1971) 1589;
<https://doi.org/10.1088/0022-3727/4/10/319>
- [39] Acar FZ, Buyukbas-Ulusan A, Tataroglu A (2018) J Mater Sci: Mater Electron 29(15):12553-12560; <https://doi.org/10.1007/s10854-018-9371-y>
- [40] A. Buyukbas-Ulusan and A. Tataroglu Journal of Materials Science: Materials in Electronics volume 31, pages 9888-9893 (2020); <https://doi.org/10.1007/s10854-020-03533-1>
- [41] Yilmaz, M.; Demir, Y.; Aydoğan, S.; Grilli, M.L. Energies 2021, 14, 7983;
<https://doi.org/10.3390/en14237983>
- [42] M. Cakar, N. Yildirim, S. Karatas, C. Temirci, A. Turut, J. Appl Phys. 100 (2006) 074505;
<https://doi.org/10.1063/1.2355547>
- [43] S.R. Forrest, M.L. Kaplan, P.H. Schmidt, J. Appl. Phys. 60 (1986) 2406;
<https://doi.org/10.1063/1.337153>
- [44] Aydoğan S, İncekara Ü, Deniz AR, Türüt A (2010) Microelectron Eng 87(12):2525-2530;
<https://doi.org/10.1016/j.mee.2010.06.004>

- [45] P. Stallinga, H.L. Gomes, H. Rost, A.B. Holmes, M.G. Harrison, and R.H. Friend, *J. Appl. Phys.* 89, 1713 (2001); <https://doi.org/10.1063/1.1334634>
- [46] I. T. Zedan, F. M. A. El-Taweel, R. A. N. Abu El-Enein, H. H. Nawar & E. M. El-Menyawy, *Journal of Electronic Materials* volume 45, pages5928-5935 (2016)
- [47] Güllü, Ö, Aydoğan, Ş, Türüt, A. (2012). *Thin Solid Films*, 520(6), 1944-1948; <https://doi.org/10.1016/j.tsf.2011.09.043>